Tropospheric distribution and variability of N_2O: Evidence for strong tropical emissions

E. A. Kort,[1] P. K. Patra,[2] K. Ishijima,[2] B. C. Daube,[1] R. Jiménez,[3] J. Elkins,[4] D. Hurst,[4,5] F. L. Moore,[4,5] C. Sweeney,[4,5] and S. C. Wofsy[1]

Received 5 April 2011; revised 10 May 2011; accepted 16 May 2011; published 6 August 2011.

[1] Measurements of atmospheric N_2O spanning altitudes from the surface to 14 km, and latitudes from 67°S to 85°N, show high concentrations in the tropics and subtropics, with strong maxima in the middle and upper troposphere. The pattern varies significantly over time scales of a few weeks. Global simulations do not accurately capture observed distributions with latitude, altitude, or time. Inversion results indicate strong, episodic inputs of nitrous oxide from tropical regions (as large as 1 Tg N-N_2O over 9 weeks) are necessary to produce observed vertical and latitudinal distributions. These findings highlight strong tropical sources of N_2O with high temporal variability, and the necessity of using full vertical profile observations in deriving emissions from atmospheric measurements. **Citation:** Kort, E. A., P. K. Patra, K. Ishijima, B. C. Daube, R. Jiménez, J. Elkins, D. Hurst, F. L. Moore, C. Sweeney, and S. C. Wofsy (2011), Tropospheric distribution and variability of N_2O: Evidence for strong tropical emissions, *Geophys. Res. Lett.*, *38*, L15806, doi:10.1029/2011GL047612.

1. Introduction

[2] In the last 40 years, increasing concern has developed over humanity's role in affecting atmospheric constituents and resulting consequences. Two areas in particular have garnered much attention from scientists and policy makers alike: stratospheric ozone depletion and global warming. Quantification of climatically relevant trace gas emissions is crucial in both understanding the severity of the problem, and for defining emissions regulations. Using only reported statistics and/or biogeochemical models (so called 'bottom-up' methods) to gauge emissions have severe limitations, and the need for direct atmospheric observations ('top-down' methods) to quantify emissions has been made explicit [*Nisbet and Weiss*, 2010].

[3] Top-down approaches take different forms. Regional studies, typically of limited spatial and/or temporal scale, have employed total column [*Wunch et al.*, 2009], surface [*Thompson et al.*, 2010], satellite [*Bergamaschi et al.*, 2007], and aircraft observations [*Kort et al.*, 2008; *D'Amelio et al.*, 2009]. Global studies make use of data from surface stations and/or satellite observations to invert for surface fluxes, with aircraft data typically only used for post-inversion comparisons [*Stephens et al.*, 2007; *Chevallier et al.*, 2010] due to limited spatial and temporal coverage, with a recent exception where upper tropospheric data are used in an inversion [*Patra et al.*, 2011]. These post-inversion analyses [*Stephens et al.*, 2007; *Patra et al.*, 2011] have demonstrated that in-situ vertical profiles can contain crucial additional information regarding fluxes.

[4] Here we present in-situ, global scale, surface to stratosphere observations of Nitrous oxide (N_2O) collected on the first two HIAPER Pole to Pole Observations campaigns (HIPPO) conducted in January 2009 and November 2009. Nitrous oxide, presently the single most important anthropogenically emitted stratospheric ozone depleting substance (ODS) [*Ravishankara et al.*, 2009], is the third most potent long-lived anthropogenic greenhouse gas (http://www.esrl.noaa.gov/gmd/aggi/). In spite of the important role N_2O plays in our atmosphere [*Forster et al.*, 2007], and the continuously increasing atmospheric burden (0.5–0.8 ppb/year on ~322 ppb (2009); www.esrl.noaa.gov/gmd/hats/combined/N2O.html), our understanding of sources (natural and anthropogenic), their distribution, strength, and seasonality remain poorly quantified due to the lack of in-situ data with adequate resolution and spatial-temporal coverage.

[5] Global [*Prinn et al.*, 1990; *Hirsch et al.*, 2006; *Huang et al.*, 2008] top-down studies of emissions point to increased northern tropical emissions and decreased southern ocean fluxes compared to current inventories [*Huang et al.*, 2008], but are derived from only surface observations with limited spatial and temporal coverage, particularly in tropical and southern regions. The reliance on surface observations perhaps explains why regional studies [*Nevison et al.*, 2004; *Kort et al.*, 2008, 2010] disagree with global analyses for northern mid-latitudes, finding prior inventories are too low with a significant seasonal component.

[6] With the HIPPO observations we have repeatedly observed enhanced N_2O at altitude (5–14 km) on 3.5 independent transects spanning the remote Pacific Ocean from the Arctic to the Antarctic. Results indicate that strong bursts of tropical emissions are a significant contributor to global nitrous oxide fluxes, and highlight the importance of obtaining full, in-situ tropospheric profiles.

2. Model and Measurements

[7] Atmospheric N_2O simulations are performed with the Center for Climate System Research/National Institute for

[1]School of Engineering and Applied Science and Department of Earth and Planetary Sciences, Harvard University, Cambridge, Massachusetts, USA.
[2]Environmental Biogeochemical Cycle Research Program, Research Institute for Global Change, Japan Agency for Marine-earth Science and Technology, Yokohama, Japan.
[3]Air Quality Research Group, Department of Chemical and Environmental Engineering, Universidad Nacional de Colombia, Bogota, Colombia.
[4]NOAA Earth System Research Laboratory, Boulder, Colorado, USA.
[5]Cooperative Institute for Research in Environmental Sciences, University of Colorado at Boulder, Boulder, Colorado, USA.

0094-8276/11/2011GL047612

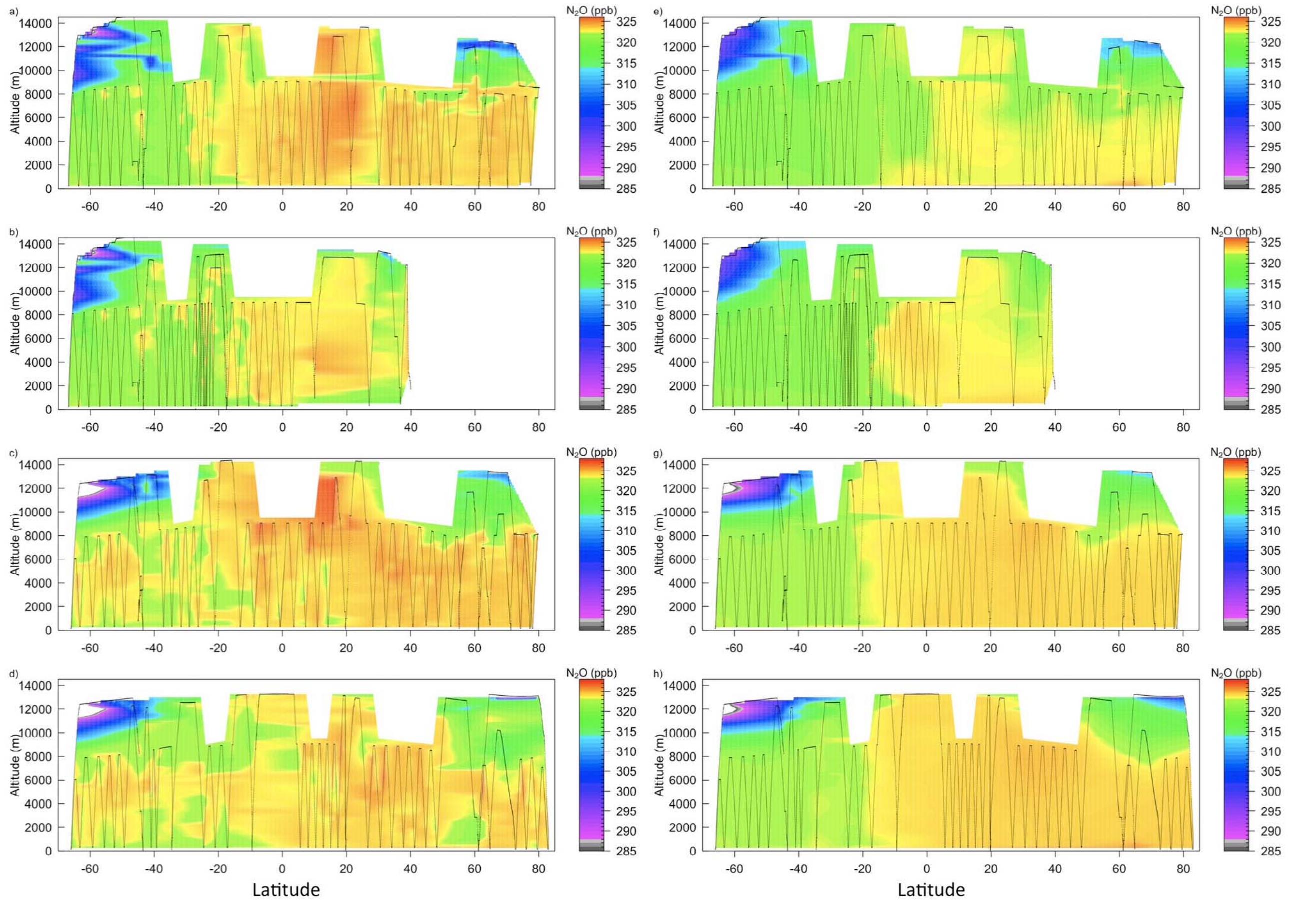

Figure 1. Latitudinal and vertical distributions of N_2O along HIPPO-1 (January 2009) and 2 (November 2009) transects. (a) HIPPO-1 Southbound (SB) observations. (b) HIPPO-1 Northbound (NB) observations. (c) HIPPO-2 SB observations. (d) HIPPO-2 NB observations. (e) HIPPO-1 SB model. (f) HIPPO-1 NB model. (g) HIPPO-2 SB model. (h) HIPPO-2 NB model. Flight tracks in black lines.

Environmental Studies/Frontier Research Center for Global Change (CCSR/NIES/FRCGC) atmospheric general circulation based chemistry-transport model (ACTM), as outlined by *Ishijima et al.* [2010]. The horizontal model resolution is T42 spectral truncation (~2.8° × 2.8°) with 67 sigma-pressure vertical layers from the earth's surface to 90 km. Model transport is nudged towards horizontal winds and temperature from JRA-25 at 6-hourly time intervals [*Onogi et al.*, 2007].

[8] Stratospheric losses from photolysis and oxidation reactions are explicitly modeled. Prior emissions are composed of EDGAR4.1 (Emission Database for Global Atmospheric Research, release version 4.1. http://edgar.jrc/ec/europa.eu, 2010) for anthropogenic emissions (4.3 TgN yr^{-1}). Monthly mean ocean fluxes are from *Jin and Gruber* [2003] (3.5 TgN yr^{-1}), and annual natural soil fluxes are from EDGAR 2, scaled by a factor of 1.6 to 10.5 TgN yr^{-1}. This scaling of the soil fluxes works well to capture a realistic trend of modeled tropospheric N_2O by balancing the total emissions (18.3 TgN yr^{-1}) and the stratospheric sink [*Ishijima et al.*, 2010]. Sulfur Hexafluoride (SF_6) was modeled also with ACTM using EDGAR4.1 emission distribution for 2005, with global totals following *Levin et al.* [2010] through 2008, extrapolated through 2009.

[9] N_2O measurements were made *in-situ* by the Harvard/Aerodyne Quantum Cascade Laser Spectrometer (QCLS), one of the HIAPER Airborne Instrumentation Solicitation (HIAS) suite of instruments aboard the GV, retrieved at 1-Hz with 1σ precision of 0.09 ppb and accuracy of 0.2 ppb on the NOAA2006 scale [*Hall et al.*, 2007] (0.03% and 0.06% at 320 ppb, see auxiliary material).[1] SF_6 measurements were made *in-situ* every 70 s by the Unmanned aircraft systems Chromatograph for Atmospheric Trace Species (UCATS) 2-channel gas chromatograph with accuracy and precision of 1%.

3. Results and Discussion

[10] Due to its long lifetime (~120 years) [*Forster et al.*, 2007], the distribution of N_2O is fairly uniform with relatively small variability in the troposphere (3–5 ppb superimposed on a background of ~322 ppb in 2009; Figures 1a–1d). Global model results produce somewhat similar features (Figures 1e–1h), but measurements show notable enhancements at altitude in the tropics and subtropics, first seen on HIPPO-1 [cf. *Wofsy et al.*, 2011], not present in the simulations. These enhancements are persistent features of four cross-sections, two obtained in January 2009, and two in November 2009, but with notable variability even on southbound and

[1] Auxiliary material files are available in the HTML. doi:10.1029/2011GL047612.

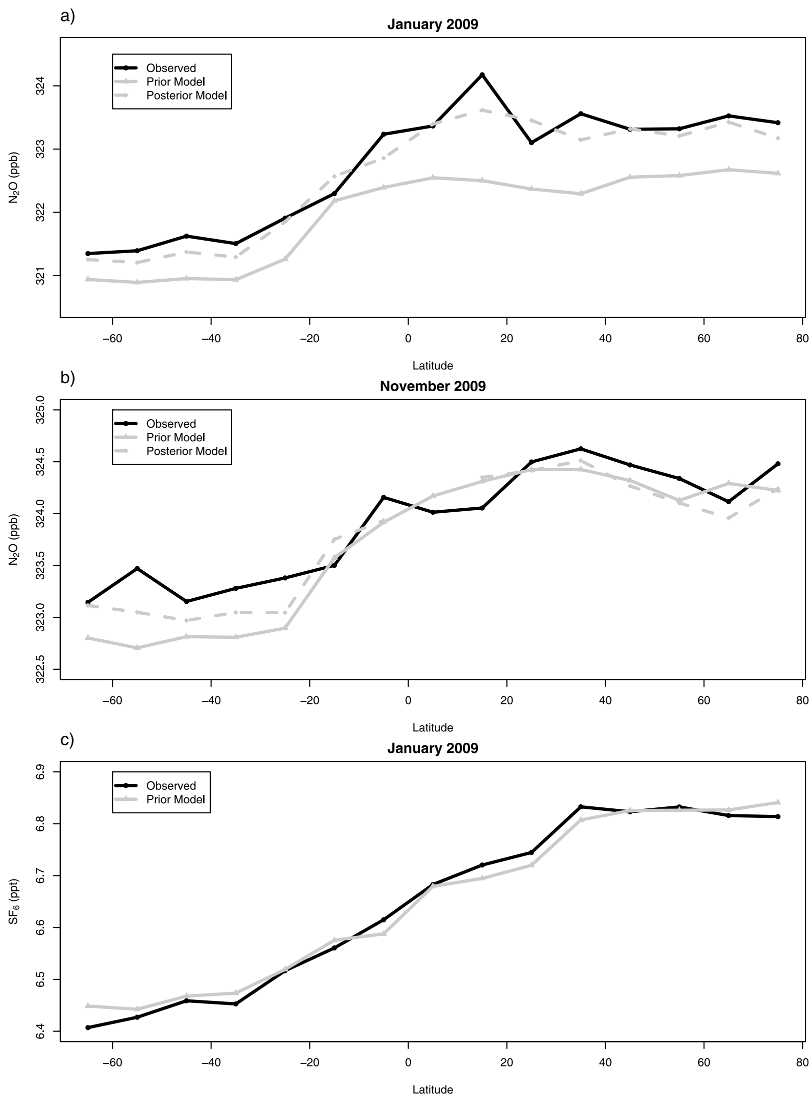

Figure 2. Latitudinal gradients of pressure-weighted column averages. Observations (solid black line), prior model (solid gray line), and optimized model (dashed gray line) for (a) HIPPO-1 and (b) HIPPO-2. (c) Observations (black) and prior (gray) model for HIPPO-1 SF_6.

northbound legs only separated by days or weeks. Evidently, global-scale sources of N_2O have strong temporal variability not represented in current models.

[11] Model-data comparison enables quantification of information gained with the full tropospheric measurements compared to surface observations. For the purpose of comparing with model output, we bin our observations in 10 degree latitudinal and 500 m vertical bins. Model output is sampled along the flight tracks, and aggregated in the same manner. For HIPPO-1, simulation results agree well with QCLS near-surface observations, so no bias is adjusted in the inverse analysis. For HIPPO-2, the model shows a negative bias relative to QCLS near-surface observations (due to either a model growth rate mismatch or calibration offset), so a tropospheric bias of 1.2 ppb is removed.

[12] First we consider only data collected from 250–750 m, representing remote surface observations typically used in inversion studies. Latitudinal gradients in the prior model closely match the observed surface layer in both HIPPO-1 (Figure S5a of the auxiliary material) and HIPPO-2. We performed a Bayesian inversion using just the 0–1 km data, solving for 12 global regions (similar to *Huang et al.* [2008]) for three different three week time frames, starting six weeks before mission start (pulse 1), three weeks before mission start (pulse 2), and simultaneous with mission start (pulse 3) (see auxiliary material for inversion details). With the excellent prior agreement, resultant regional emissions changes are found to be small, with little to no statistical significance, and produce optimized model output little changed from the prior.

[13] Applying the identical approach instead using the full tropospheric profile results in different conclusions. In spite of excellent agreement found at the surface, modeled HIPPO-1 total column does not match observations in three ways (Figure 2a): 1) Simulations have a low bias. 2) The latitudinal gradient is too small in the model. 3) Enhanced values in northern tropics/sub-tropics are missing. Inversion results produce large changes from prior emissions fields and better reproduce the observed total column (Figure 2a). A fairly even increase to global emissions addresses the

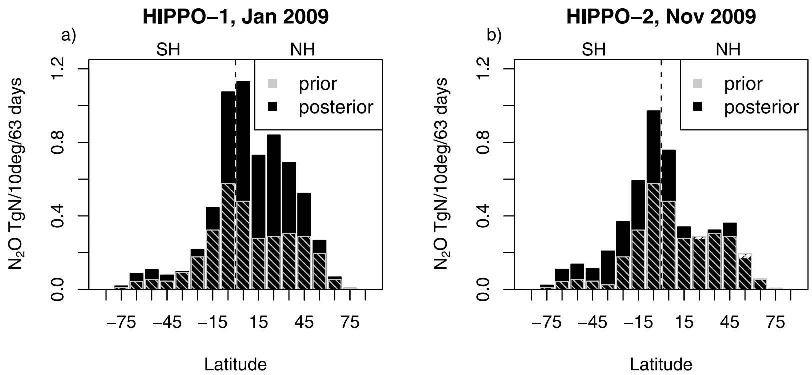

Figure 3. Latitudinal distribution of prior and posterior emissions for (a) HIPPO-1 and (b) HIPPO-2.

bias. Additional increases to tropical emissions and northern emissions (Figure 3a) correct for the latitudinal gradient, as well as reproducing the observed 'bulge' seen 0–20°N. If we corrected for the column bias prior to inverting this would reduce the global net flux increase, but increases to northern tropical and higher latitude emissions (addressing the latitudinal gradient and 'bulge') remain. Enhanced emissions are attributed by the inversion to South America, Africa, and the China/Japan/Southeast Asia regions.

[14] Results were similar for HIPPO-2: despite excellent surface model-data agreement, simulated total column results deviate from observations in two ways (Figure 2b): 1) The modeled latitudinal gradient is too strong. 2) Southern hemisphere modeled values are too low. Optimized model results better reproduce observations (Figure 2b) by increasing tropical and southern hemisphere emissions (Figure 3b). Enhanced emissions are in South America and Africa. Hence, inversion results find significantly enhanced tropical emissions in both January and November, with very different emissions patterns at higher latitudes.

[15] The large size of these adjustments, and the strong temporal variability evident in the observed cross sections, are consistent with findings of other recent top down studies (*Kort et al.*, 2008). It is clear that the enhanced N_2O seen at altitude is a product of tropical emissions lofted to the middle and upper troposphere by convection. With these observations alone we cannot distinguish whether the actual regional emissions exhibit strong temporal dynamics, winking on and off, or whether strong sources are episodically injected into the free troposphere by convective activity. These two types of variability could be coupled, as rainfall may dramatically stimulate N_2O production and release from soils, and coincident convection could loft these enhanced in N_2O air parcels to high altitude. This idea would be consistent with data from Amazon soils, where N_2O emissions were found to vary from negligible to 20 ng-N/(cm^2hr^1), stimulated by increases in soil moisture [*Keller et al.*, 2005]. This idea would also be consistent with inversion results finding strong emissions in South America in early December 2008 (pulse 1), at which time southern Brazil experienced heavy rainfall and flooding.

[16] We validated transport in the model with SF_6, a species with a relatively well-known emissions field. Comparisons of modeled column SF_6 (reduced 0.072 ppt to account for bias) with observations show excellent agreement (Figure 2c; at the time of this writing HIPPO-2 SF_6 data gaps prevent comparable comparison for November 2009). This agreement suggests model transport may be robust for simulating the total column. Considering the vertical gradient in more detail (Figure S5c of the auxiliary material), the tropical vertical gradient discrepancy present for SF_6 may be a product of over-mixing in model parameterization of convection, which might help explain the model's difficulty in representing the extent of the observed reversed vertical gradient of N_2O (Figures S5a and S5b of the auxiliary material). If we assume the entire discrepancy in the tropical SF_6 vertical gradient was caused by transport errors (0.1 ppt between 500 & 4500 m), and map this 'error' into N_2O space by comparing to latitudinal gradients (~0.4 ppt SF_6, ~2 ppb N_2O), this apparent over-mixing could be responsible for the model underestimating N_2O at altitude by 0.5 ppb, in line with the *optimized* model discrepancy, but it could not explain the multiple ppb offset in the prior model. Thus transport error does not appear to be the major driver of deviance in the prior model.

[17] Elevated N_2O at altitude has previously been seen by CARIBIC from flask samples in monsoonal outflow [*Schuck et al.*, 2010]. The defining features of N_2O data illustrated here are validated both by instances of coincident enhancement of independent tracers, and overall validation comparing QCLS observations with flask samples over multiple missions (Figure S3 of the auxiliary material), though the magnitude of enhancement of individual features in HIPPO-1 is captured only by the continuous 1-Hz observations of QCLS.

4. Conclusion

[18] Our analysis demonstrates that surface observations remote from sources alone cannot be used for inverse modeling of global N_2O emissions, that global sources are concentrated in the tropics, at least in November and January, and that emissions are highly variable on weekly time scales. It appears that large-scale convective activity lofts enhanced in N_2O air parcels to altitudes ranging 2 to 14 km, from sources over tropical land. Rainfall concurrent with convection may increase tropical soil N_2O production [*Keller et al.*, 2005], amplifying variability in the mid-troposphere. Inverse studies using the ACTM suggest that South America and Africa are large, variable emission sources in both Northern Hemisphere fall and winter (0–5× prior emissions). The region encompassing China, Japan, and Southeast Asia appeared to have very large emissions in January (3–5× prior emissions), possibly a signal of strong agricultural emissions.

Future, continuous, high-precision observations in the tropical source regions would be invaluable in distinguishing between variability in emissions and transport, and enable more accurate estimations of annual N_2O emissions.

[19] **Acknowledgments.** E.A.K. acknowledges financial support from the Department of Defense through the NDSEG fellowship program. HIPPO was supported by NSF grants ATM-0628575, ATM-0628519, ATM-0628388, and by the National Center for Atmospheric Research (NCAR). NCAR is supported by the NSF. We thank the pilots, mechanics, technicians, and scientific crew working on HIPPO. We thank Xin Jin for providing oceanic flux model results. This work is partly supported by JSPS/MEXT KAKENHI-A grant 22241008. Participation by NOAA instruments was supported in part by the NSF through its Atmospheric Chemistry Program to CIRES, NOAA through its Atmospheric Composition and Climate Program and the Office of Oceanic and Atmospheric Research, and NASA through its Upper Atmosphere Research Program and Radiation Sciences Program.

[20] The Editor thanks two anonymous reviewers for their assistance in evaluating this paper.

References

Bergamaschi, P., et al. (2007), Satellite cartography of atmospheric methane from SCIAMACHY onboard ENVISAT: 2. Evaluation based on inverse model simulations, *J. Geophys. Res.*, *112*, D02304, doi:10.1029/2006JD007268.

Chevallier, F., et al. (2010), CO_2 surface fluxes at grid point scale estimated from a global 21 year reanalysis of atmospheric measurements, *J. Geophys. Res.*, *115*, D21307, doi:10.1029/2010JD013887.

D'Amelio, M. T. S., L. V. Gatti, J. B. Miller, and P. Tans (2009), Regional N_2O fluxes in Amazonia derived from aircraft vertical profiles, *Atmos. Chem. Phys.*, *9*(22), 8785–8797, doi:10.5194/acp-9-8785-2009.

Forster, P., et al. (2007), Changes in atmospheric constituents and in radiative forcing, in *Climate Change 2007: The Physical Science Basis. Contribution of Working Group I to the Fourth Assessment Report of the Intergovernmental Panel on Climate Change*, edited by S. Solomon et al., Cambridge Univ. Press, Cambridge.

Hall, B. D., G. S. Dutton, and J. W. Elkins (2007), The NOAA nitrous oxide standard scale for atmospheric observations, *J. Geophys. Res.*, *112*, D09305, doi:10.1029/2006JD007954.

Hirsch, A. I., A. M. Michalak, L. M. Bruhwiler, W. Peters, E. J. Dlugokencky, and P. P. Tans (2006), Inverse modeling estimates of the global nitrous oxide surface flux from 1998–2001, *Global Biogeochem. Cycles*, *20*, GB1008, doi:10.1029/2004GB002443.

Huang, J., et al. (2008), Estimation of regional emissions of nitrous oxide from 1997 to 2005 using multinetwork measurements, a chemical transport model, and an inverse method, *J. Geophys. Res.*, *113*, D17313, doi:10.1029/2007JD009381.

Ishijima, K., et al. (2010), Stratospheric influence on the seasonal cycle of nitrous oxide in the troposphere as deduced from aircraft observations and model simulations, *J. Geophys. Res.*, *115*, D20308, doi:10.1029/2009JD013322.

Jin, X., and N. Gruber (2003), Offsetting the radiative benefit of ocean iron fertilization by enhancing N_2O emissions, *Geophys. Res. Lett.*, *30*(24), 2249, doi:10.1029/2003GL018458.

Keller, M., R. Varner, J. D. Dias, H. Silva, P. Crill, and R. C. de Oliveira (2005), Soil-atmosphere exchange of nitrous oxide, nitric oxide, methane, and carbon dioxide in logged and undisturbed forest in the Tapajos National Forest, Brazil, *Earth Interact.*, *9*, 1–28.

Kort, E. A., et al. (2008), Emissions of CH_4 and N_2O over the United States and Canada based on a receptor-oriented modeling framework and COBRA-NA atmospheric observations, *Geophys. Res. Lett.*, *35*, L18808, doi:10.1029/2008GL034031.

Kort, E. A., et al. (2010), Atmospheric constraints on 2004 emissions of methane and nitrous oxide in North America from atmospheric measurements and a receptor-oriented modeling framework, *J. Integr. Environ. Sci.*, 125–133, *7*(2), doi:10.1080/19438151003767483.

Levin, I., et al. (2010), The global SF6 source inferred from long-term high precision atmospheric measurements and its comparison with emission inventories, *Atmos. Chem. Phys.*, *10*, 2655–2662, doi:10.5194/acp-10-2655-2010.

Nevison, C. D., T. J. Lueker, and R. F. Weiss (2004), Quantifying the nitrous oxide source from coastal upwelling, *Global Biogeochem. Cycles*, *18*, GB1018, doi:10.1029/2003GB002110.

Nisbet, E., and R. Weiss (2010), Top-down versus bottom-up, *Science*, *328*(5983), 1241–1243, doi:10.1126/science.1189936.

Onogi, K., et al. (2007), The JRA-25 reanalysis, *J. Meteorol. Soc. Jpn.*, *85*, 369–432, doi:10.2151/jmsj.85.369.

Patra, P. K., Y. Niwa, T. J. Schuck, C. A. M. Brenninkmeijer, T. Machida, H. Matsueda, and Y. Sawa (2011), Carbon balance of South Asia constrained by passenger aircraft CO_2 measurements, *Atmos. Chem. Phys. Discuss.*, *11*, 5379–5405, doi:10.5194/acpd-11-5379-2011.

Prinn, R., D. Cunnold, R. Rasmussen, P. Simmonds, F. Alyea, A. Crawford, P. Fraser, and R. Rosen (1990), Atmospheric emissions and trends of nitrous-oxide deduced from 10 years of ALE-GAGE data, *J. Geophys. Res.*, *95*, 18,369–18,385, doi:10.1029/JD095iD11p18369.

Ravishankara, A. R., J. S. Daniel, and R. W. Portmann (2009), Nitrous oxide (N_2O): The dominant ozone-depleting substance emitted in the 21st century, *Science*, *326*(5949), 123–125, doi:10.1126/science.1176985.

Schuck, T. J., C. A. M. Brenninkmeijer, A. K. Baker, F. Slemr, P. F. J. von Velthoven, and A. Zahn (2010), Greenhouse gas relationships in the Indian summer monsoon plume measured by the CARIBIC passenger aircraft, *Atmos. Chem. Phys.*, *10*, 3965–3984, doi:10.5194/acp-10-3965-2010.

Stephens, B. B., et al. (2007), Weak northern and strong tropical land carbon uptake from vertical profiles of atmospheric CO_2, *Science*, *316*(5832), 1732–1735, doi:10.1126/science.1137004.

Thompson, R. L., C. Gerbig, and C. Rodenbeck (2010), A Bayesian inversion estimate of N_2O emissions for western and central Europe and the assessment of aggregation errors, *Atmos. Chem. Phys. Discuss.*, *10*, 26,073–26,115, doi:10.5194/acpd-10-26073-2010.

Wofsy, S. C., et al. (2011), HIAPER Pole-to-Pole Observations (HIPPO): Fine grained, global scale measurements for determining rates for transport, surface emissions, and removal of climatically important atmospheric gases and aerosols, *Philos. Trans. R. Soc. A*, *369*, 2073–2086, doi:10.1098/rsta.2010.0313.

Wunch, D., P. O. Wennberg, G. C. Toon, G. Keppel-Aleks, and Y. G. Yavin (2009), Emissions of greenhouse gases from a North American megacity, *Geophys. Res. Lett.*, *36*, L15810, doi:10.1029/2009GL039825.

B. C. Daube, E. A. Kort, and S. C. Wofsy, School of Engineering and Applied Science and Department of Earth and Planetary Sciences, Harvard University, Cambridge, MA 02138, USA.

J. Elkins, D. Hurst, F. L. Moore, and C. Sweeney, NOAA Earth System Research Laboratory, 325 Broadway, Boulder, CO 80305, USA.

K. Ishijima and P. K. Patra, Environmental Biogeochemical Cycle Research Program, Research Institute for Global Change, Japan Agency for Marine-earth Science and Technology, 3173-25 Showa-machi, Kanazawa-ku, Yokohama 236-0001, Japan.

R. Jiménez, Air Quality Research Group, Department of Chemical and Environmental Engineering, Universidad Nacional de Colombia, Bogota DC 111321, Colombia.